Observational Study

Medicine®

OPEN

The correlation between the microstructure of meibomian glands and ocular *Demodex* infestation

A retrospective case-control study in a Chinese population

Shengnan Cheng, MD, Mingchang Zhang, MD, Hua Chen, MSc, Wanlin Fan, MSc, Yukan Huang, MD*

Abstract

Meibomian gland dysfunction (MGD) is a common disease in ophthalmic clinic. This study aimed to explore ocular *Demodex* infestation on the microstructure changes of the meibomian glands (MGs) in patients with MGD by in vivo confocal microscopy (IVCM).

We retrospectively reviewed 103 eyes of 52 patients with MGD and 62 eyes of 31 non-MGD patients. All enrolled patients underwent IVCM examination. The following IVCM parameters were recorded: the MG acinar density (MAD), MG acinar longest diameter (MALD), MG acinar shortest diameter (MASD), MG orifice area (MOA), severity of MG fibrosis (MF), MG acinar irregularity (MAI), meibum secretion reflectivity (MSR), inhomogeneous appearance of walls of acinar units (AWI) and periglandular interstices of acinar units (API), and the number of *Demodex*.

The positive rate of *Demodex* infestation in MGDs was 89.32%, and statistically higher than control group (controls; $P < .001$). All parameters showed statistically significant differences between MGDs and controls ($P < .001$), and *Demodex*-negative group and *Demodex*-positive group ($P < .05$) in both MGDs and controls, except MAD ($P = .826$) in controls. The number of *Demodex* was positively correlated with MALD, MASD, MF, MAI, MSR, AWI, and API in MGDs and controls ($P < .05$), and negatively correlated with MAD and MOA in MGDs ($P < .05$). MOA showed a strong significant correlation with the number of *Demodex* in controls ($P < .001$), whereas there was no significant difference between the number of *Demodex* and the MAD in controls ($P = .448$).

Demodex can cause microstructural changes of MGs, which can cause or aggravate MGD, and the more the number of *Demodex* infestation, the more serious the structural damage.

Abbreviations: API = inhomogeneous appearance of periglandular interstices of acinar units, AWI = inhomogeneous appearance of walls of acinar units, controls = control group, IVCM = in vivo confocal microscopy, MAD = MG acinar density, MAI = MG acinar irregularity, MALD = MG acinar longest diameter, MASD = MG acinar shortest diameter, MF = severity of MG fibrosis, MG = meibomian gland, MGD = meibomian gland dysfunction, MOA = MG orifice area, MSR = meibum secretion reflectivity.

Keywords: correlation, *Demodex*, meibomian glands, meibomian glands dysfunction, microstructure

1. Introduction

Meibomian gland dysfunction (MGD) represents a common clinical eye disease and is the most common cause of dry eyes. Epidemiological studies showed that about 20% of Europeans and 60% of Asians have MGD.[1] The incidence of MGD increased with age, and the prevalence of MGD stood at 33% in people younger than 30 years and 71.7% in those aged 60 years or older.[2,3] The etiology and pathogenesis of MGD remain unclear. *Demodex* has been found to be the most common ectoparasite in human skin.[4] The infestation rate of *Demodex* is 84% in 60 years old and 100% in people older than 70 years.[5] Previous clinical studies have revealed a correlation between ocular *Demodex* infestation and MGD.[6–10] The results indicated that *Demodex* infestation is one of the important contributors to the development of MGD, but the specific pathogenesis of *Demodex* infestation is still poorly understood. Previous studies on the microstructural changes of meibomian glands (MGs) caused by *Demodex* infestation were scanty and their relationship has not been quantitatively examined.

As a noninvasive and pain-free diagnostic technique for ophthalmic examination, in vivo confocal microscopy (IVCM) is also characterized by high magnification and resolution, in-vivo, real-time, and dynamic imaging, among others. The characteristic morphology of *Demodex* can be clearly seen during microscopic observation. A number of studies have shown that the detection rate of ocular *Demodex* by IVCM is higher than the traditional eyelash microscopy.[11–13] Moreover, IVCM allows accurate observation at the cellular level, making it possible to examine the microstructural changes of MGs in vivo. Especially at the early stage of MGD, IVCM can more accurately show the

Editor: Choul Yong Park.

Funding sources: This study was supported by the National Natural Science Foundation of China (No. 81670824) and the Natural Science Foundation of Hubei Province of China (No. 2016CFB421). The funding organization had no role in the design or conduct of this study.

The authors report no conflicts of interest.

Department of Ophthalmology, Union Hospital, Tongji Medical College, Huazhong University of Science and Technology, Wuhan, China.

* Correspondence: Yukan Huang, Department of Ophthalmology, Union Hospital, Tongji Medical College, Huazhong University of Science and Technology, Jiefang Road 1277, Wuhan 430022, Hubei Province, China (e-mail: whuh_huangyk@163.com).

Medicine (2019) 98:19(e15595)

Received: 29 November 2018 / Received in final form: 12 April 2019 / Accepted: 16 April 2019

http://dx.doi.org/10.1097/MD.0000000000015595

size and morphology of the acinus of MGs, their openings and the degree of adjacent fibrosis, thereby permitting a quantitative study of their association. In this study, IVCM was employed to observe the infestation of *Demodex* in eyelash follicles and the microstructural changes of MGs, with an attempt to better understand their relationship.

2. Method

2.1. Subjects

This study was approved by the Ethics Committee of Union Hospital affiliated to Tongji Medical College, Huazhong University of Science and Technology, Wuhan, China, and was conducted in strict accordance with the Helsinki Declaration. All participants provided written informed consent.

This case-control study retrospectively reviewed the medical records of 83 consecutive patients (including 165 eyes) who had been seen between September to November 2017 in the Department of Ophthalmology of Union Hospital. Among them, 52 consecutive patients with MGD (involving 103 eyes) were selected. Another 31 non-MGD patients (including 62 eyes), matched for age and sex, were included as control group (controls), among whom 131 eyes were positive for *Demodex* infestation and 34 eyes were negative for *Demodex* infestation. After taking a routine history, all patients underwent a complete eye examination and photographic documentation of the entire ocular surface, including microstructural of MGs and the number of *Demodex* infestation by IVCM. MGD was diagnosed according to the criteria previously summarized by Tomlinson et al.[14] Exclusion criteria included eye or body suffering from acute inflammation; being on local (e.g., eye drops or eye ointment) or systemic medication; having ocular trauma, ocular deformity scar, exophthalmos, eyelid insufficiency, ocular surface diseases, and other inflammatory eye diseases; having undergone eye surgery within 3 months; having diabetes mellitus, rheumatism, immune diseases, and other serious systemic diseases; wearing corneal contact lens on the day of examination; and patients younger than 18 years.

2.2. Image acquisition of in vivo confocal microscopy

IVCM was performed on all subjects with the Rostock Corneal Module Heidelberg Retina Tomograph III (HRTIII Cornea Module; Heidelberg Engineering GmbH, Dossenheim, Germany). The detection magnification was 800 times and the axial resolution was 1 μm. Oxybuprocaine hydrochloride eye drops (Santen Pharmaceutical Co, Ltd, Japan) were instilled into the conjunctival sac before examination. After adjusting the instrument and setting the parameters, a fixed light rendered the patient's eyeballs turn downward, which prevents the rotation of the patient's eyeballs during image collection. The upper eyelid was flipped, to fully expose the eyelash root, palpebral margin, and MG. The lens was pushed to make the upper eyelid margin of the patient in contact with the sterile cap. Then the focus plane and depth were adjusted. Scanning started from the root of the eyelash to the palpebral margin and the MG. At the same time, parallel scanning was performed from the nasal lateral side to the temporal side. The root of 3 eyelashes and their follicles were scanned along the nasal side, the center, and the temporal side in turn, with 9 eyelashes were taken in total.

2.3. Image analysis of in vivo confocal microscopy

In this study, the parameters of MGs and *Demodex* in eyelash follicles of upper eyelid were determined and were subjected to statistical analysis. The MG acinus, orifice of excretory duct, and the infestation of *Demodex* in the hair follicles of the root of eyelashes were examined, and the corresponding images were collected and stored. Three nonoverlapping, high-quality IVCM images of MGs were randomly selected from the nasal, central, and temporal sides of the upper eyelid (a total of 9 images per eyelid). The following variables were quantitatively determined: MG acinar density (MAD) (the acinus manually marked inside each $400 \times 400\,\mu m$ frame and the density was automatically calculated using HRT3 cell counting system), MG acinar longest diameter (MALD), MG acinar shortest diameter (MASD), MG orifice area (MOA) (the area was calculated automatically by ImageJ software, developed by Wayne Rasband, National Institutes of Health, Bethesda, MD), severity of MG fibrosis (MF), MG acinar irregularity (MAI), meibum secretion reflectivity (MSR), inhomogeneous appearance of walls (AWI), and periglandular interstices of acinar units (API). The MF was scored on a 3-point scale, with no fibrosis listed as 0, fibrosis in less than half of the lower eyelid as 1 and fibrosis in more than half of the lower eyelid as 2.[15] The MSR was evaluated on a 4-point scale, as reported in a previous study from Villani et al,[16] with black color of secretion listed as 0, dark gray color as 1, light gray color as 2, and white color as 3. The inhomogeneity of interstices or walls of acinar units was rated on a 4-point scale, with absence of punctate reflecting elements listed as 0, minimal presence of punctuate reflecting elements as 1, moderate presence as 2, and heavy presence as 3. The MAI was assessed on a 4-point scale, with virtually round or elliptical shape as 0, minimal presence of lobulated-shaped acinar units as 1, moderate presence as 2, and heavy presence as 3.[16,17] The total number of *Demodex* infestation at the root of 9 eyelashes was calculated. The result was taken as negative when the number was <3 and as positive the when the number was ≥ 3.

2.4. Statistical analysis

All statistical analyses were performed by using SPSS software package (Version 23.0, SPSS Inc, Chicago, IL). The binocular data were included in the statistical analysis (one MGD patient was 1-eyed and the only 1 eye was included). The data of the test results were expressed in $x \pm s$. For comparison of MAD, MALD, MASD, and MOA, the number of *Demodex* and age matching, independent sample t test was employed. For comparison of positive rate of *Demodex* between 2 groups, sex matching, Chi-square test was used. For comparison of scores between 2 groups, such as scores of MF, MAI, MSR, AWI, and API, Mann-Whitney test was used. Pearson and Spearman correlation analysis was used for the analysis of the relationship between the number of *Demodex* and microstructural parameters. All confidence intervals were set at 95%, and a $P < .05$ was considered to be statistically significant.

3. Results

3.1. General analysis of patients

In this retrospective study, 83 patients (involving 165 eyes) were enrolled. Of them, 52 patients (involving 103 eyes) clinically diagnosed with MGD (28 woman, 24 men) were aged 23 to 85 years (average age 52.15 ± 16.20 years). Correspondingly, 31

sex- and age-matched controls (62 eyes) (15 woman, 16 men) were 18 to 73 years old (average age 45.64 ± 14.75 years). There existed no differences in sex and age between patients with MGD and controls ($P = .071$ and .630, respectively).

3.2. Comparison of positive rate of Demodex infestation

IVCM scan can show the structure of eyelash follicles and the number of *Demodex* in the follicles (Fig. 1). In MGD group, 92 eyes were positive for *Demodex* and 11 eyes were negative for *Demodex*, with a positive rate of 89.32%. Thirty-nine eyes were positive for *Demodex* and 23 eyes were negative for *Demodex* in 62 eyes of controls, the positive rate being 43.55%. The positive rates of *Demodex* infestation in both groups were significantly different ($P < .001$). The mean number of *Demodex* per eyelid infestation was also statistically significant ($P < .001$) (Fig. 2).

3.3. Comparison of microstructure of meibomian glands

The acinus of MGs in controls was of round, ellipsoid, or other regular shape, and arranged regularly and neatly. There was homogeneous connective tissue between the acinus, and the average scores of MAI, MSR, API, AWI, and MF narrowly ranged between 0 and 1, and a few between 1 and 2. The orifices of the excretory ducts were round, and their inner wall was smooth, presenting low reflection, with no obvious fibrosis around it. Accordingly, the MG acinus was dilated, fused, and atrophied, with decreased density in MGDs. The average scores of MAI, MSR, API, AWI, and MF ranged between 2 and 3, and a few between 1 and 2. The orifice of the excretory duct was irregular, and the inner wall was not smooth. The area of orifice became smaller, and most of them were obstructed by moderated- and high-reflectance substances, with fibrosis developing in adjacent tissue. The mean values of the MAD and MOA in MGDs were significantly lower than in the controls ($P < .001$). The mean values of the MALD, MASD, MF, MAI, MSR, API, and AWI in MGDs were significantly higher than in controls ($P < .001$) (Table 1).

IVCM can well show the differences of microstructure of MGs between the *Demodex*-negative groups (DNs) and *Demodex*-positive groups (DPs) (Fig. 3). All parameters showed statistically significant differences between DNs and DPs

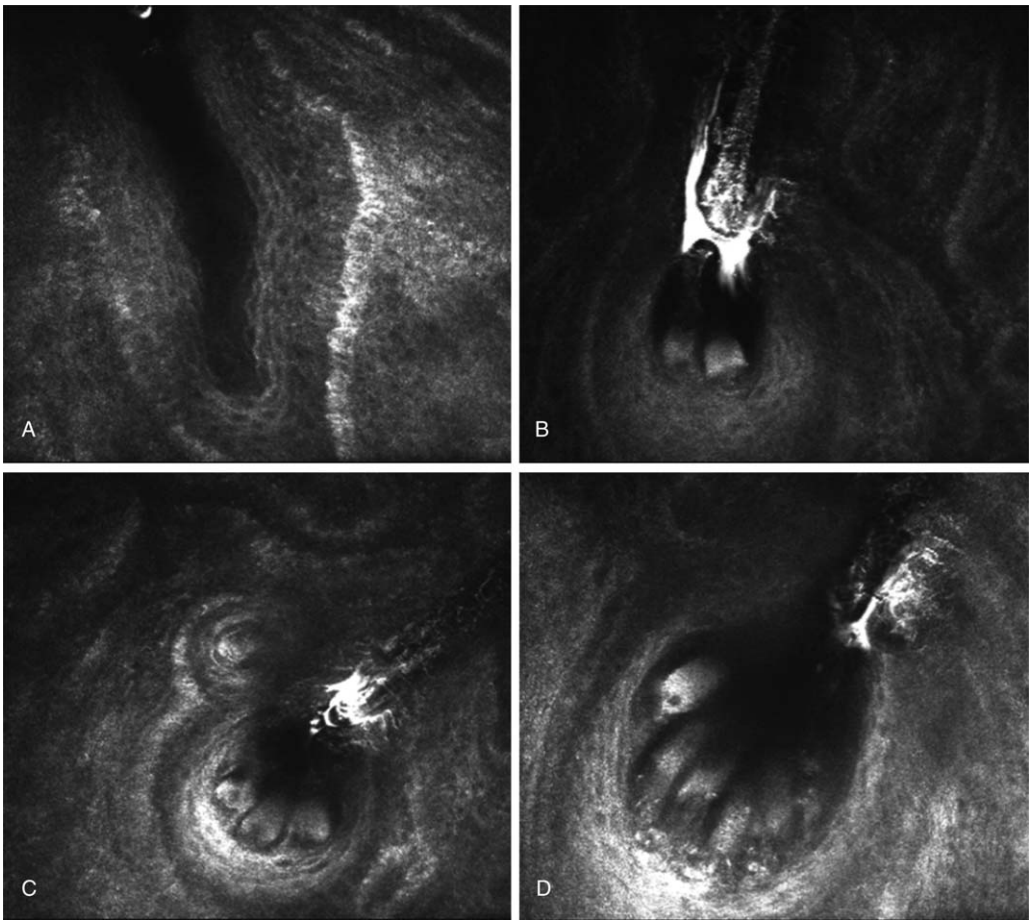

Figure 1. Observation of *Demodex* infestation in mascara follicles using in vivo confocal microscopy (IVCM). A, The hair follicle of uninfected with *Demodex* mites was morphologically uniform and had low reflectance, and the hair follicle is structurally intact. B, Two fusiform *Demodex* mites can be seen in the hair follicle, with the head of the hair follicle having slight fibrosis and a large amount of grease secretion being attached to the root of the eyelash at the end of the hair follicle. C, The hair follicle was located next to the gland, and there are 3 short rod-like *Demodex* in it. The tissues in the head of the hair follicle and the adjacent glands had obvious fibrosis and a small amount of grease-like secretion were attached to the end of the cilia. D, The hair follicles were evidently dilated, containing 5 long columnar mites and 1 short fusiform *Demodex*. A large number of piecemeal secretions were found in the head of the hair follicles, with hair follicles having obvious fibrosis and destruction of various degrees. (images: 400 × 400 mm; magnification: ×800 times).

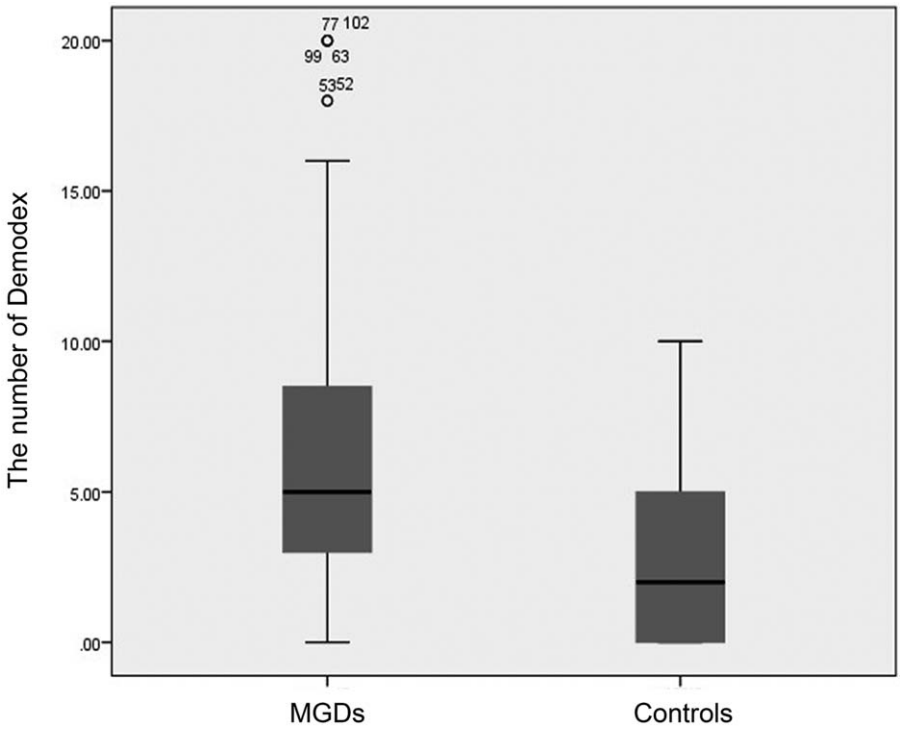

Figure 2. Comparison of the number of *Demodex* in meibomian gland dysfunctions (MGDs) and controls. The mean number of *Demodex* per eyelid infestation in MGDs (6.50±5.01) was significantly higher than in controls (2.82±2.91), and the difference was statistically significant ($P < .001$).

($P < .05$) in both MGDs and controls, except MAD ($P > .05$) in controls (Table 2).

3.4. Correlation between the number of Demodex and the morphological parameters of meibomian glands

The number of *Demodex* was negatively correlated with MAD and MOA ($P < .05$), and positively correlated with MALD, MASD, MF, MAI, MSR, AWI, and API ($P < .05$) in MGDs. Similarly, the number of *Demodex* was negatively correlated with MOA ($P < .05$), but not MAD ($P > .05$), and positively correlated with MALD, MASD, MF, MAI, MSR, AWI, and API ($P < .05$) in controls (Fig. 4).

Table 1

Comparison of microstructure of meibomian glands between meibomian gland dysfunction group and control group.

Parameters	MGDs	Controls	*P*
MAD, glands/mm^2 (mean±SD)	92.74±34.80	115.66±37.14	<.001
MOA, μm^2 (mean±SD)	1287.63±790.19	4041.79±1088.36	<.001
MALD, μm (mean±SD)	153.50±36.26	58.36±20.62	<.001
MASD, μm (mean±SD)	56.94±23.15	27.48±10.23	<.001
MAI (mean±SD)	2.20±0.80	1.23±0.71	<.001
MSR (mean±SD)	2.21±0.65	1.26±0.70	<.001
API (mean±SD)	2.43±0.69	1.52±0.70	<.001
AWI (mean±SD)	2.12±0.88	0.97±0.75	<.001
MF (mean±SD)	1.23±0.51	0.37±0.55	<.001

API = inhomogeneous appearance of periglandular interstices of acinar units, AWI = inhomogeneous appearance of walls of acinar units, controls = control group, MAD = MG acinar density, MAI = MG acinar irregularity, MALD = MG acinar longest diameter, MASD = MG acinar shortest diameter, MF = severity of MG fibrosis, MGDs = Meibomian gland dysfunction group, MOA = MG orifice area, MSR = meibum secretion reflectivity.

4. Discussion

Demodex was one of the most common parasites in the human body. In the eye, *Demodex* infestation was believed to be one of the factors responsible for chronic blepharitis, conjunctivitis, and MGD.[18] Mechanistically, *Demodex* infestation caused MGD may via 4 mechanisms: mechanical stimulation of *Demodex* resulted in obstruction of hair follicles and sebaceous glands, thereby causing epithelial hyperplasia, hyperkeratosis, and hair follicle dilatation; *Demodex* was a carrier of bacteria, such as streptococcus, staphylococcus, cholera bacilli, and can also spread viruses and fungi; bacterial antigens on the surface of *Demodex* mite can induce inflammatory reaction in host, while bacteria in parasite-infected intestine can stimulate the proliferation of monocytes in peripheral blood of infected patients; the metabolites of *Demodex*, the cytoskeleton of mites, and its cleavage can cause damage to host tissues.[5,19–23] Although there were many kinds of *Demodex*, but only *Demodex folliculorum* and *Demodex brevis* were found in the human body. Adult *D folliculorum* measures 279 to 294 μm long and the arrowhead eggs was 104 μm × 41 μm in size. *D folliculorum* was mainly found in the eyelash follicles, mostly in clusters, principally causing anterior blepharitis. *D brevis* was smaller (165–208 μm in length) and their eggs are of fusiform shape (60 × 34 μm). *D brevis* was usually found deep in the MG duct and the sebaceous glands of the lash, mostly living alone, and mainly resulting in posterior blepharitis. The current detection techniques were not accurate enough for the detection of *Demodex* in the MG duct and IVCM was unable to distinguish the 2 species of *Demodex*. Therefore, in this study we only examined the infestation of *Demodex* in eyelash hair follicles.

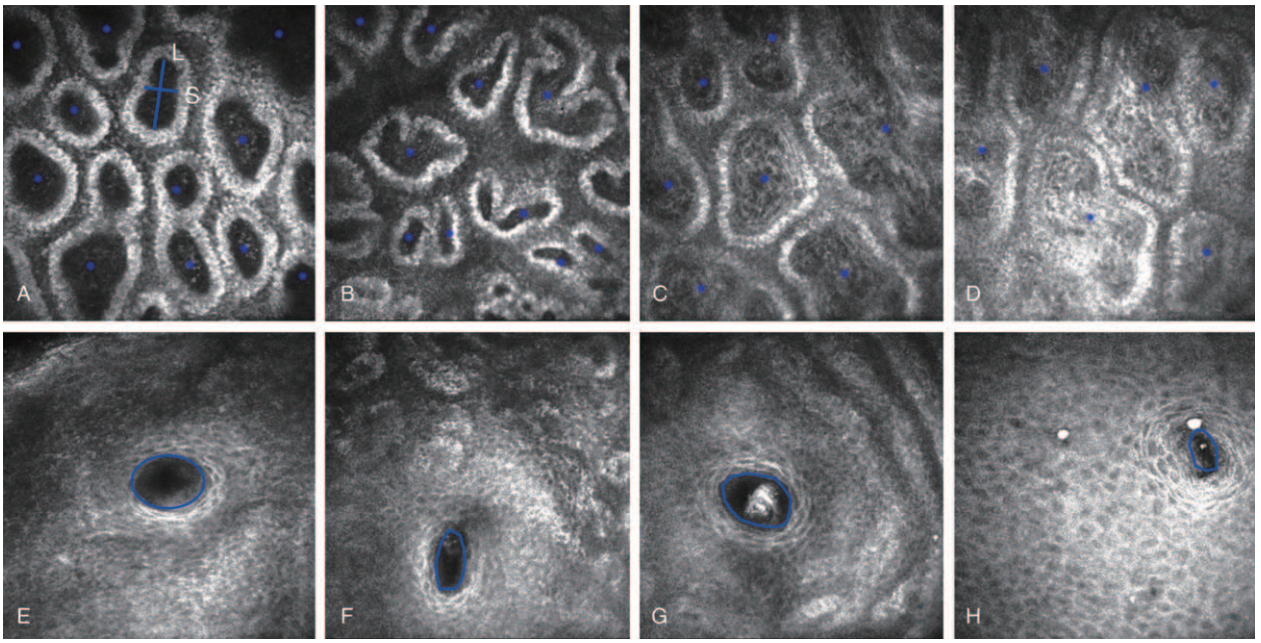

Figure 3. Microstructural morphology of the acinus and the orifice of excretory duct in meibomian glands (MGs) by in vivo confocal microscopy. A, E: Controls with DNs. It can be seen that the acinus was oval, with the MAI and MSR being rated 0, the AWI and API 1, and were arranged neatly, with connective tissues being evenly distributed in the acinus. The MAD was about 120 glands/mm^2, the MALD was 82.57 μm, and the MASD was 38.08 μm. The orifice of the excretory duct was round, and the interior was uniform and presented low reflection, with an area of about 5026 μm^2. B, F: Controls with DPs: The acinus was relatively irregular, and slightly dilated and fused, with the MAI, MSR, AWI and API being rated 1. The MAD was about 90 glands/mm^2, the MALD was 114.04 μm, and the MASD was 44.05 μm. The orifice of the excretory duct was vertically oval, with its interior density being uneven, surrounding tissues developing fibrosis, its area measuring about 2617 μm^2. C, G: MGDs with DNs. The acinus was obviously dilated and disorderly arranged, with their internal and external density being uneven. The MAI, MSR, AWI, and API was rated 2. The MAD was about 61 glands/mm^2, the MALD was 142.56 μm and the MASD was 89.45 μm. The orifice of the excretory duct was irregular in shape, with obvious blockage by high-reflection materials and partial fibrosis around it, with an area of about 4729 μm^2. D, H: MGDs with DPs. The shape of the acinus was extremely irregular, some of the acinar structure disappeared, and the MAI, MSR, AWI, and API was graded 3. The MAD was about 39 glands/mm^2, the MALD was 202.36 μm, and the MASD was 97.01 μm. The orifice of the excretory ducts was petal-like and shrank, with an area of about 1093 μm^2. API = inhomogeneous appearance of periglandular interstices of acinar units, AWI = inhomogeneous appearance of walls of acinar units, controls = control group, DNs = *Demodex*-negative group, DPs = *Demodex*-positive group, MAD = MG acinar density, MAI = MG acinar irregularity, MALD = MG acinar longest diameter, MASD = MG acinar shortest diameter, MF = severity of MG fibrosis, MGDs = meibomian gland dysfunction group, MOA = MG orifice area, MSR = meibum secretion reflectivity. (images: 400 × 400 mm; magnification: ×800 times).

Traditional method for the detection of *Demodex* in mascara follicles mainly depends on the extraction of mascara samples, which were observed directly under optical microscope. It was difficult to detect *Demodex* in MG and deep hair follicles by eyelash extraction, and counting deviation may result. Moreover, the eyelash extraction, to a certain extent, caused discomfort or pain to patients and tended to reduce the compliance of patients. Multiple studies employed IVCM for the detection of *Demodex* hair follicles. The detection rate and reliability of *Demodex* hair follicle were shown to be higher than those of traditional methods.[11–13,24] This study, using IVCM to detect *Demodex* in mascara follicles, also yielded similar results. Many studies had

Table 2

Comparison of microstructure of meibomian glands between *Demodex*-negative group and *Demodex*-positive group.

	MGDs (n = 103), mean ± SD			Controls (n = 62), mean ± SD		
Parameters	**DNs (n = 11)**	**DPs (n = 92)**	***P***	**DNs (n = 35)**	**DPs (n = 27)**	***P***
MAD, glands/mm^2	116.55 ± 40.34	89.89 ± 33.19	.016	114.74 ± 37.80	116.85 ± 36.96	.826
MOA, μm^2	2056.27 ± 577.25	1195.73 ± 763.75	<.001	4397.83 ± 934.01	3580.26 ± 1116.44	.003
MALD, μm	120.83 ± 22.66	157.41 ± 35.68	<.001	46.07 ± 15.77	74.29 ± 14.34	<.001
MASD, μm	33.82 ± 9.82	59.71 ± 22.75	<.001	22.84 ± 7.57	33.49 ± 10.19	<.001
MAI	1.64 ± 0.81	2.27 ± 0.77	.014	1.03 ± 0.57	1.48 ± 0.80	.018
MSR	1.45 ± 0.69	2.30 ± 0.59	<.001	0.89 ± 0.53	1.74 ± 0.59	<.001
API	1.27 ± 0.47	2.57 ± 0.58	<.001	1.20 ± 0.58	1.93 ± 0.62	<.001
AWI	1.09 ± 0.54	2.24 ± 0.83	<.001	0.74 ± 0.61	1.26 ± 0.81	.010
MF	0.91 ± 0.54	1.27 ± 0.49	.036	0.06 ± 0.24	0.78 ± 0.58	<.001

API = inhomogeneous appearance of periglandular interstices of acinar units, AWI = inhomogeneous appearance of walls of acinar units, controls = control group, DNs = *Demodex*-negative group, DPs = *Demodex*-positive group, MAD = MG acinar density, MAI = MG acinar irregularity, MALD = MG acinar longest diameter, MASD = MG acinar shortest diameter, MF = severity of MG fibrosis, MGDs = meibomian gland dysfunction group, MOA = MG orifice area, MSR = meibum secretion reflectivity.

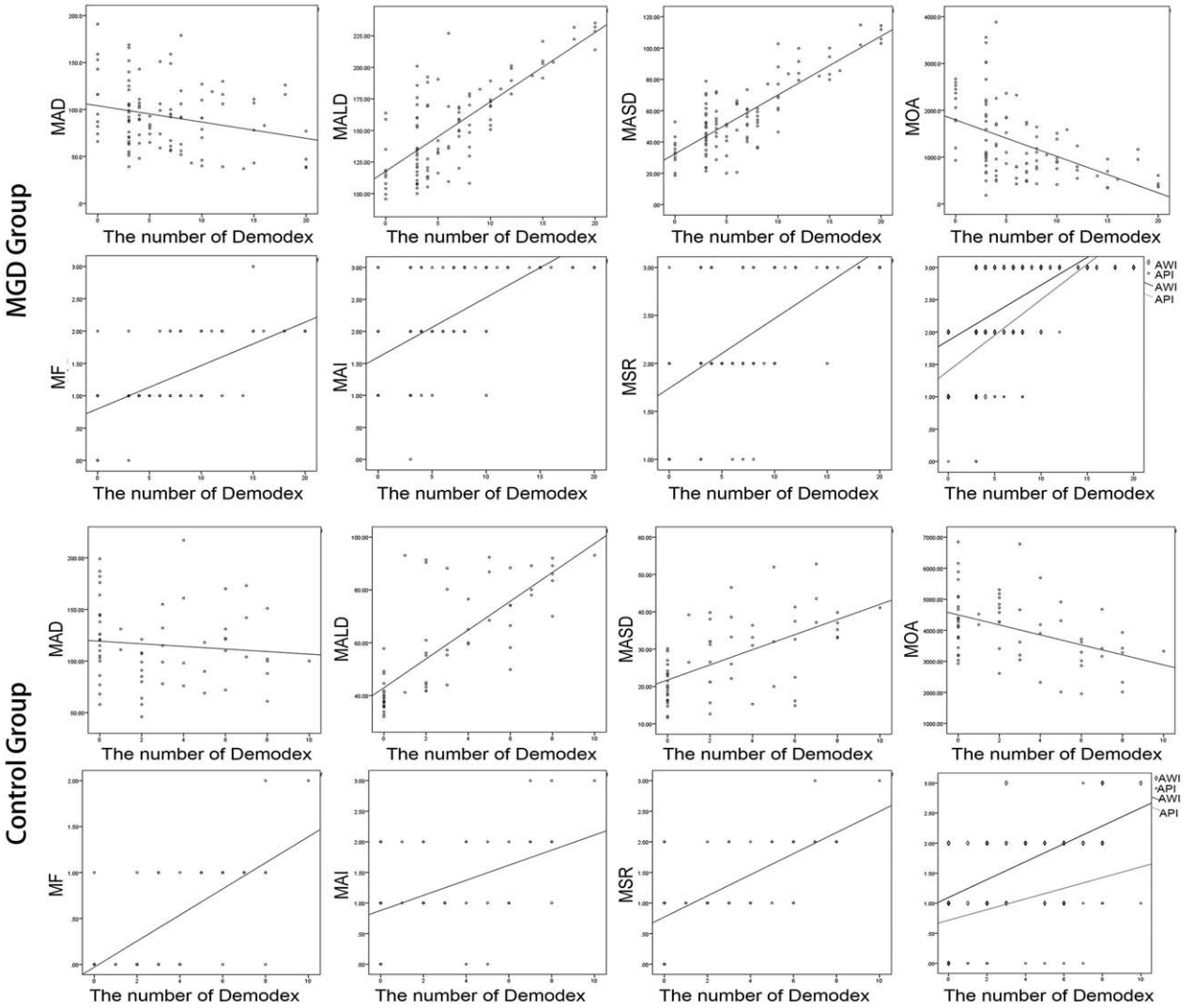

Figure 4. The correlation analysis between the number of *Demodex* and the microstructural parameters of MGs in MGDs and controls. The number of *Demodex* was negatively correlated with MAD and MOA ($P < .05$), and positively correlated with MALD, MASD, MF, MAI, MSR, AWI, and API in MGDs. The number of *Demodex* was negatively correlated with MOA ($P < .05$), rather than MAD ($P > .05$), and positively correlated with MALD, MASD, MF, MAI, MSR, AWI, and API ($P < .05$) in controls ($P < .05$). API = inhomogeneous appearance of periglandular interstices of acinar units, AWI = inhomogeneous appearance of walls of acinar units, MAD = MG acinar density, MAI = MG acinar irregularity, MALD = MG acinar longest diameter, MASD = MG acinar shortest diameter, MF = severity of MG fibrosis, MOA = MG orifice area, MSR = meibum secretion reflectivity.

shown that the infestation rate of *Demodex* in normal population was 20% to 80%, and the average density of *Demodex* in skin was $\leq 5/cm^2$.[25,26] However, there was no international standard or consensus on the clinical diagnosis of ocular *Demodex* infestation, whether by eyelash extraction or IVCM. The *Demodex*-positive diagnostic criteria used in this study were based on the consensus of Chinese experts, which was mentioned on the first Chinese Ocular Surface and Tear Film Diseases Congress and the third Chinese Dry Eye Congress in Changsha, Hunan, China. In our series, the positive rate of *Demodex* infestation in hair follicles, as detected by IVCM, was 89.32%, which was significantly higher than that of controls (43.55%). The number of *Demodex* per eyelid in MGDs was significantly higher than that in controls, suggesting that the infestation of *Demodex* in hair follicles was closely related to the development of MGD.

Previous studies using IVCM to observe the morphology of MGs showed that the MG acinus and the MG orifice of excretory duct were abnormal in patients with MGD, with accompanying acinar inflammatory cell infiltration, fibrosis, and other changes.[27–29] Randon et al, on the basis of IVCM findings, proposed a new classification for MGD in terms of the microstructural changes of MGs in patients with dry eye. The classification can serve as guidelines for the clinical diagnosis and treatment.[30] In this study, we found that the mean values of the MAD and MOA were significantly lower in MGDs than in the controls ($P < .001$), and the mean values of the MALD, MASD, MF, MAI, MSR, API, and AWI were significantly higher in MGDs than in controls ($P < .001$), which suggests that the aforementioned parameters could be used as quantitative measures for the diagnosis of MGD. Ibrahim et al found that the sensitivity and specificity of MALD, MASD and MAD were 90% and 81%, 86% and 96%, 81% and 81%,

respectively.[31] This study, however, did not examine the specificity and sensitivity of the diagnostic measures, which are the targets of our future studies. We also found that there existed statistically significant differences in all parameters between DNs and DPs in MGDs. Our study suggested that *Demodex* infestation can enlarge MALD and MASD, reduce MAD, and the number of MGs per unit area, resulting in decreased lipid secretion by the MGs. At the same time, the movement of *Demodex* in and out of the excretory duct and its activities in the glandular duct can cause mechanical damage to the acinus and the orifice of the excretory duct. Repeated inflammatory stimulation and injury repair can result in epithelium keratosis, fibrosis, and even scar formation of the orifice. As a consequence, the orifice area of the excretory duct was decreased and the lipid excretion from the gland was also reduced. Fibrosis and keratosis in the opening of the gland also aggravated due to *Demodex*-induced inflammatory stimulation, which leading to a decreased tenacity of the gland, and thus reducing its lipid transportation ability. When the tenacity dropped to a point where it cannot overcome the resistance of lipid transport, the lipid cannot be excreted from the gland, resulting in functional disorder, even obstruction of the excretory duct. Further development of the condition would cause dilation and shrinkage of the MG acinus, thereby further reducing the acinar density and aggravating the MAI, MSR, AWI, and API. Furthermore, the function of MGs might be impaired or lost altogether, thereby leading to a vicious circle and eventually the development of MGD. Our study showed that the number of *Demodex* infestation in MGDs was negatively correlated with MAD and MOA, and was positively correlated with MALD, MASD, MF, MAI, MSR, AWI, and API. The results suggested that the degree of damage to the microstructure of MGs was positively correlated with the number of *Demodex* infestation, and the more the number of *Demodex*, the more serious the damage, indicating that the accumulation of *Demodex* was also an important factor responsible for the difference in the degree of ultrastructural damage of MGs. Moreover, we also found that the mean values of MOA in the DPs were significantly lower than in the DNs, and the mean values of the MALD, MASD, MF, MAI, MSR, API, and AWI in DPs were significantly higher than in DNs of controls, and there was a significant correlation between the number of *Demodex* mites and the aforementioned parameters, which further demonstrated that *Demodex* might cause structural damage to the MGs. There was, however, no significant difference in MAD between the DNs and DPs of controls, and the correlation between MAD and the number of *Demodex* in controls not statistically significant either. But the number of *Demodex* infestation in MGDs was significantly higher than that in controls. Therefore, we are led to speculate that *Demodex* infestation may need to reach a certain number to effect a reduction in the acinar density, which belongs to the early stage of disease development.

To sum up, our study demonstrated that the microstructure of MGs and the status of *Demodex* infestation in mascara follicles can be observed by IVCM, which can help us to better understand the role of *Demodex* in the pathogenesis of MGD, which is essential for further etiological study and treatment of MGD.

Acknowledgments

The authors thank Huatao Xie of Department of Ophthalmology, Union Hospital, Tongji Medical College, Huazhong University of Science and Technology for his guidance and help in this study.

Author contributions

Conceptualization: Shengnan Cheng, Mingchang Zhang, Yukan Huang.
Data curation: Shengnan Cheng, Hua Chen, Wanlin Fan, Yukan Huang.
Formal analysis: Shengnan Cheng.
Funding acquisition: Yukan Huang.
Investigation: Shengnan Cheng, Hua Chen, Wanlin Fan.
Project administration: Yukan Huang.
Supervision: Mingchang Zhang, Yukan Huang.
Writing – original draft: Shengnan Cheng, Yukan Huang.
Writing – review and editing: Mingchang Zhang, Yukan Huang.
Yukan Huang orcid: 0000-0002-3163-6883.

References

[1] Schaumberg DA, Nichols JJ, Papas EB, et al. The international workshop on meibomian gland dysfunction: report of the subcommittee on the epidemiology of, and associated risk factors for, MGD. Invest Ophthalmol Vis Sci 2011;52:1994–2005.
[2] Kobayashi A, Yokogawa H, Sugiyama K. In vivo laser confocal microscopy of Bowman's layer of the cornea. Ophthalmology 2006;113: 2203–8.
[3] Nichols KK, Foulks GN, Bron AJ, et al. The international workshop on meibomian gland dysfunction: executive summary. Invest Ophthalmol Vis Sci 2011;52:1922–9.
[4] Murube J. Demodex hominis. Ocul Surf 2015;13:181–6.
[5] Liu J, Sheha H, Tseng SC. Pathogenic role of Demodex mites in blepharitis. Curr Opin Allergy Clin Immunol 2010;10:505–10.
[6] Alver O, Kıvanç SA, Budak BA, et al. A clinical scoring system for diagnosis of ocular demodicosis. Med Sci Monit 2017;23:5862–9.
[7] Lee SH, Chun YS, Kim JH, et al. The relationship between demodex and ocular discomfort. Invest Ophthalmol Vis Sci 2010;51: 2906–11.
[8] Nicholls SG, Oakley CL, Tan A, et al. Demodex treatment in external ocular disease: the outcomes of a Tasmanian case series. Int Ophthalmol 2016;36:691–6.
[9] Zhang XB, Ding YH, He W. The association between demodex infestation and ocular surface manifestations in meibomian gland dysfunction. Int J Ophthalmol 2018;11:589–92.
[10] Randon M, Liang H, El Hamdaoui M, et al. In vivo confocal microscopy as a novel and reliable tool for the diagnosis of Demodex eyelid infestation. Br J Ophthalmol 2015;99:336–41.
[11] Sattler EC, Maier T, Hoffmann VS, et al. Noninvasive in vivo detection and quantification of Demodex mites by confocal laser scanning microscopy. Br J Dermatol 2012;167:1042–7.
[12] Slutsky JB, Rabinovitz H, Grichnik JM, et al. Reflectance confocal microscopic features of dermatophytes, scabies, and demodex. Arch Dermatol 2011;147:1008.
[13] Longo C, Pellacani G, Ricci C, et al. In vivo detection of Demodex folliculorum by means of confocal microscopy. Br J Dermatol 2012; 166:690–2.
[14] Tomlinson A, Bron AJ, Korb DR, et al. The international workshop on meibomian gland dysfunction: report of the diagnosis subcommittee. Invest Ophthalmol Vis Sci 2011;52:2006–49.
[15] Ban Y, Ogawa Y, Ibrahim OMA, et al. Morphologic evaluation of meibomian glands in chronic graft-versus-host disease using in vivo laser confocal microscopy. Mol Vis 2011;17:2533–43.
[16] Villani E, Beretta S, De Capitani M, et al. In vivo confocal microscopy of meibomian glands in Sjogren's syndrome. Invest Ophthalmol Vis Sci 2011;52:933–9.
[17] Lin T, Gong L. In vivo confocal microscopy of meibomian glands in primary blepharospasm: a prospective case-control study in a Chinese population. Medicine (Baltimore) 2016;95:e3833.
[18] Kheirkhah A, Blanco G, Casas V, et al. Fluorescein dye improves microscopic evaluation and counting of demodex in blepharitis with cylindrical dandruff. Cornea 2007;26:697–700.
[19] Lacey N, Kavanagh K, Tseng SC. Under the lash: Demodex mites in human diseases. Biochem (Lond) 2009;31:2–6.
[20] Kim JH, Chun YS, Kim JC. Clinical and immunological responses in ocular demodecosis. J Korean Med Sci 2011;26:1231–7.

[21] Filho PA, Hazarbassanov RM, Grisolia AB, et al. The efficacy of oral ivermectin for the treatment of chronic blepharitis in patients tested positive for Demodex spp. Br J Ophthalmol 2011;95:893–5.
[22] Raszeja-Kotelba B, Jenerowicz D, Izdebska JN, et al. Some aspects of the skin infestation by Demodex folliculorum [in Polish]. Wiad Parazytol 2004;50:41–54.
[23] Huang Y, He H, Sheha H, et al. Ocular demodicosis as a risk factor of pterygium recurrence. Ophthalmology 2013;120:1341–7.
[24] Jalbert I, Rejab S. Increased numbers of Demodex in contact lens wearers. Optom Vis Sci 2015;92:671–8.
[25] Elston DM. Demodex mites: facts and controversies. Clin Dermatol 2010;28:502–4.
[26] Gerber PA, Kukova G, Buhren BA, et al. Density of Demodex folliculorum in patients receiving epidermal growth factor receptor inhibitors. Dermatology 2011;222:144–7.
[27] Fasanella V, Agnifili L, Mastropasqua R, et al. In vivo laser scanning confocal microscopy of human meibomian glands in aging and ocular surface diseases. BioMed Res Int 2016;2016:7432131.
[28] Matsumoto Y, Sato EA, Ibrahim OM, et al. The application of in vivo laser confocal microscopy to the diagnosis and evaluation of meibomian gland dysfunction. Mol Vis 2008;14:1263–71.
[29] Zhao H, Chen JY, Wang YQ, et al. In vivo confocal microscopy evaluation of meibomian gland dysfunction in dry eye patients with different symptoms. Chin Med J (Engl) 2016;129:2617–22.
[30] Randon M, Liang H, Abbas R, et al. A new classification for meibomian gland diseases with in vivo confocal microscopy [in French]. J Fr Ophtalmol 2016;39:239–47.
[31] Ibrahim OM, Matsumoto Y, Dogru M, et al. The efficacy, sensitivity, and specificity of in vivo laser confocal microscopy in the diagnosis of meibomian gland dysfunction. Ophthalmology 2010;117:665–72.